Characterization of aqueous lower polarity solvation shells around amphiphilic TEMPO radicals in water

Johannes Hunold, Jana Eisermann, Martin Brehm and Dariush Hinderberger*

Solvation of the stable nitroxide radicals 2,2,6,6-Tetramethylpiperidine-1-oxyl (TEMPO) and 4-Oxo-2,2,6,6-tetramethylpiperidine-1-oxyl (TEMPONE) in water and THF is studied in detail. With multifrequency electron paramagnetic resonance (EPR) spectroscopy at X- and Q-band as well as spectral simulations, the existence of pure water shells enclosing TEMPO in aqueous solution that lead to significantly reduced local polarity at the nitroxide moiety is shown. These aqueous lower polarity solvation shells (ALPSS) offer TEMPO a local polarity that is similar to that in organic solvents like THF. Furthermore, using double electron-electron resonance (DEER) spectroscopy, local enrichment and inhomogenous distribution without direct molecular encounters of dissolved TEMPO in water is found that can be correlated with potentially attractive interactions mediated through ALPSS. However, no local enrichment of TEMPO is found in organic solvents such as THF. In contrast to TEMPO, the structurally very similar nitroxide radical TEMPONE shows no ALPSS encapsulation behavior with water molecules in aqueous solutions. Ensemble-averaging methods such as dynamic light scattering (DLS) and electrospray ionization mass spectrometry (ESI MS) substantiate the EPR spectroscopically obtained results of ALPSS-encased TEMPO and attractive interactions between them leading to higher local concentration. Furthermore, force field molecular dynamics simulations and metadynamics deliver support for our conclusions.

Introduction

Since isolation of the first stable organic nitroxide radical in 1959, nitroxides have developed into one of the most important class of stable radicals. Nitroxides at the present time have numerous applications in many areas of chemistry and biology as well as biochemistry.[1–7] Especially in the field of electron paramagnetic resonance (EPR) spectroscopy, which depends on the presence of unpaired electron spins, nitroxide radicals have been established as so-called spin probes and spin labels in the 1970s. 2,2,6,6-Tetramethylpiperidine-1-oxyl (TEMPO) and its derivatives are well suited for investigating the self-organization of macromolecular systems (e.g. nanoscale inhomogeneities in polymers), as they can probe different regions depending on size and polarity.[8,9] Both, the size and the degree of amphiphilic character can be influenced at comparative ease by varying the structural unit in 4-position of the piperidine ring, which makes a large variety of structurally different spin probes accessible and thus allows their use for various purposes.[10] Nitroxides, like TEMPO, play a fundamental role in controlled radical polymerization reactions (e.g. nitroxide-mediated polymerization, NMP) or are often used as polarization/energy transfer agents in magnetic resonance hyperpolarization methods such as dynamic nuclear polarization (DNP) to improve NMR signal intensity.[11–13]

Especially in this context, detailed knowledge about the solvation behavior of nitroxides and their radical distribution, for example in aqueous media, is indispensable not only for possible biomedical applications, but also for the general investigation of complex supramolecular systems such as polymers or proteins.

In this paper, the behavior of the stable nitroxide radicals TEMPO and 4-Oxo-2,2,6,6-tetramethylpiperidine-1-oxyl (TEMPONE) is studied in detail by EPR spectroscopy, dynamic light scattering (DLS) and electrospray ionization mass spectrometry (ESI MS) as well as molecular and force field metadynamics simulations. The preferred ring conformation of both nitroxide radicals is displayed in Chart 1.

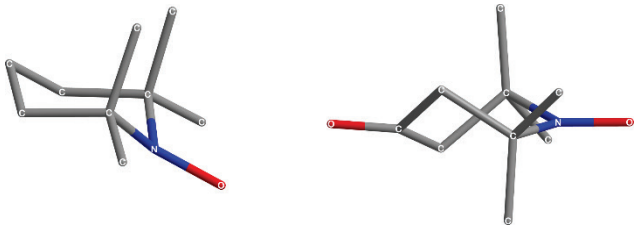

Chart 1 Structural formula with preferred ring conformation of the two investigated nitroxide radicals TEMPO (left, chair conformation) and TEMPONE (right, twisted ring conformation) according to X-ray data.[14] For better visibility, the hydrogen atoms are not shown.

Results and Discussion

The measured CW EPR spectra of TEMPO and TEMPONE in different solvents at Q-band ($\nu \approx 34$ GHz) frequencies together with their respective simulations are shown in Fig. 1. A comparison of these Q-band spectra with the corresponding CW EPR spectra at X-band ($\nu \approx 9.4$ GHz) can be found in Fig. S3 (see ESI†).

Fig. 1A and B clearly show that the EPR spectra of amphiphilic TEMPO radicals in H_2O and D_2O reflects the spectral signature of two types of spin probes. In addition to the fully water-solvated TEMPO molecules (simulation in blue), there is another species (simulation in magenta), which has hyperfine couplings indicating much more nonpolar or hydrophobic local environments and rotational motions that are significantly slowed down. In the following, we characterize this spectral component and derive the conclusion that this spectral component very likely represents TEMPO radicals, which are enclosed by an H_2O/D_2O solvation shell of significantly lower polarity (aqueous lower polarity solvation shell, ALPSS) than bulk water. ALPSS can best be described as dynamic solvent cages that enclose TEMPO for significant amounts of time in the radical ensemble. In the very beginning, to verify that we are not chasing artifacts (this, admittedly, was our first idea when first observing the ALPSS TEMPO species), we present spectra from TEMPO radicals by different suppliers and batches, as well as a spectrum measured at a different Q-band spectrometer by colleagues not involved in this study (see Fig. S12 ESI†).

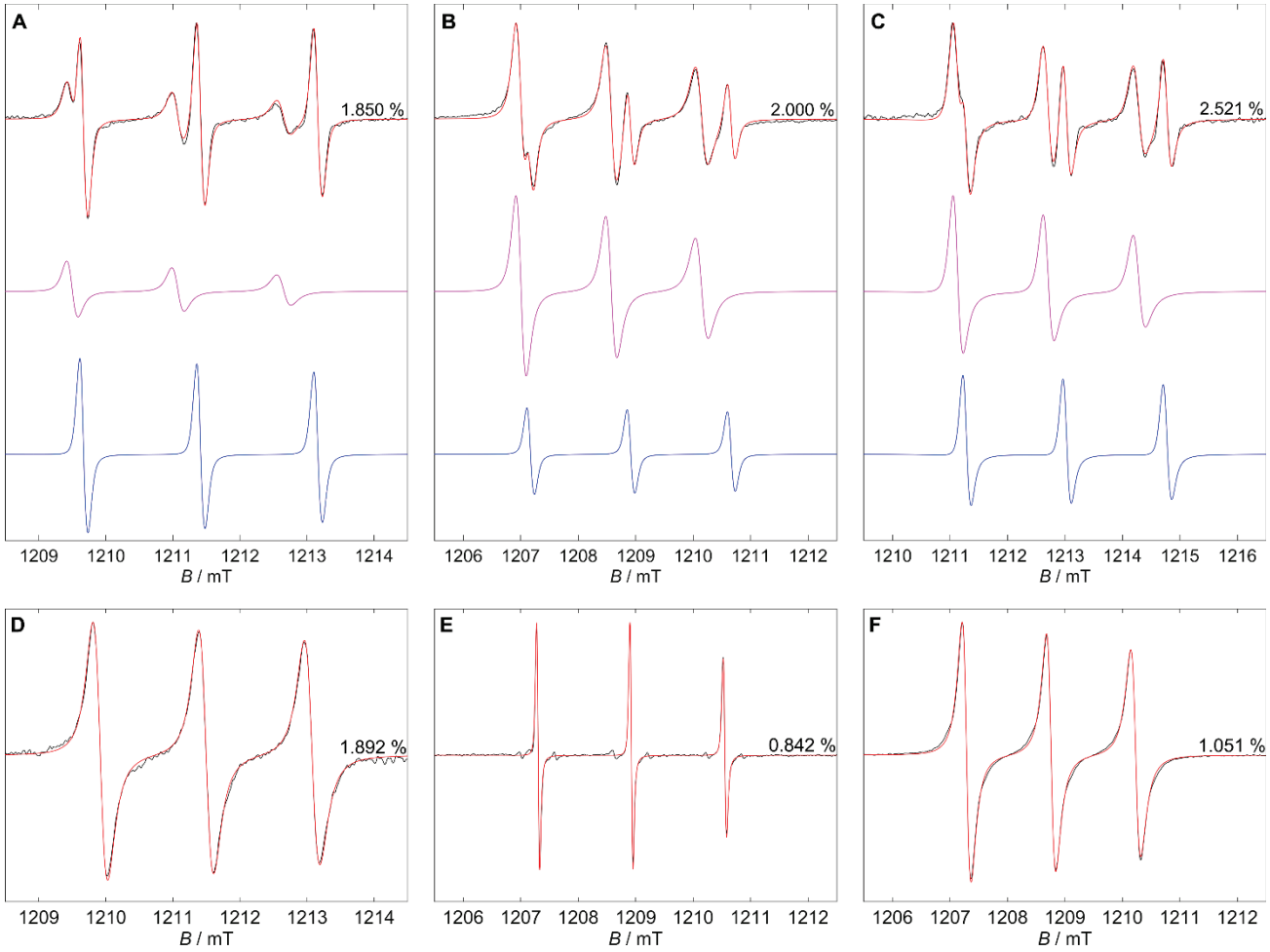

Fig. 1 Experimental Q-band ($\nu \approx 34$ GHz) CW EPR spectra (black) measured at room temperature together with their respective simulations (red) at a spin probe concentration of 0.47 mM. A) TEMPO in H_2O, B) TEMPO in D_2O and C) TEMPO in H_2O/10 vol% THF with the simulated individual spectra for the ALPSS (magenta) and hydrophilic (blue) probe species. The spectra D) TEMPO in THF, E) TEMPONE in H_2O and F) TEMPONE in THF show only one fully solvated hydrophilic spin probe species. The root-mean-square deviation (RMSD) value of each simulation is given on the right-hand side.

In pure, "classical" organic solvents like THF, however, such a second ALPSS species is not observable (see Fig. 1D). When measuring TEMPO in aqueous mixtures of THF with varying composition (see Fig. 1C and Fig. S5 ESI†), a complex behavior between the different spin probe species can be observed. With increasing THF content, the spectral fraction of the different types of spin probes changes until only fully solvated TEMPO probes in pure THF remain. This complex behavior likely stems from the strong deviation of H_2O-THF mixtures from an ideal mixing behavior.[15] Astonishingly, the addition of small amounts of THF to the aqueous solution seems to support the formation of the ALPSS TEMPO component (see Fig. 1C).

It may spectroscopically seem very surprising, that the ALPSS TEMPO species does not seem to appear in measured X-band EPR spectra (see Fig. S3 and S4 ESI†) and have not yet been reported in literature, despite showing a comparatively large spectral contrast to the fully solvated TEMPO radicals at Q-band frequencies. In fact, however, their signal at X-band (to the left of the high-field peak of the solvated TEMPO probes) is covered by the ^{13}C and ^{15}N resonance lines, which are also located in this *B*-field area and which has occluded detection of this TEMPO species. The different measurement frequencies are responsible for the observed distinct visual appearance of the ALPSS-TEMPO species in spectra at X- and Q-band. The higher *B*-field of the Q-band not only improves spectral ***g*** tensor resolution, but also enables a different view on rotational motion (as e.g. defined by the rotational correlation time τ_c) of the spin probe. In addition, also the character of the spectral line width and according relaxation rates change with frequency.[16–18] In most nitroxide radicals, the apparent line width is mainly determined by the unresolved hyperfine splitting ***A*** between the unpaired electron spin and the nuclear spins of the numerous ^1H nuclei present in its direct environment (four CH_3-groups in α-position).[19] Due to the different time scales in X- and Q-band, these unresolved hyperfine splittings have a different EPR spectroscopic effect, which is why, e.g., the spectrum of a spin probe appears somewhat slower at Q-band than at X-band at the same τ_c value. By using the software package EasySpin (see ESI† for more details regarding the spectral simulation process) the measured spectra could be simulated with identical parameters at X- and Q-band with high accuracy (see Fig. 1) by including small, unresolved hyperfine couplings in a post-convolution approach.[20] The obtained simulation parameters are summarized in Table 1.

Table 1 Isotropic Landé factor g_{iso} and hyperfine splitting constant a_{iso} as well as the spectral spin probe fraction f determined by simulation of the CW EPR spectra shown in Fig. 1.

Spectrum in Fig. 1	Probe (species)	Solvent	g_{iso}	a_{iso} / MHz	f / %
A	TEMPO (hydrophilic)	H_2O	2.00591	49.06	54.1
	TEMPO (ALPSS)		2.00648	44.27	45.9
B	TEMPO (hydrophilic)	D_2O	2.00607	49.01	16.6
	TEMPO (ALPSS)		2.00663	44.13	83.4
C	TEMPO (hydrophilic)	H_2O/ 10 vol% THF	2.00575	48.99	31.0
	TEMPO (ALPSS)		2.00629	44.22	69.0
D	TEMPO	THF	2.00655	44.37	100
E	TEMPONE	H_2O	2.00580	45.61	100
F	TEMPONE	THF	2.00626	41.33	100

A look at the simulation data in Table 1 shows that the g_{iso} and a_{iso} values of the ALPSS TEMPO probes in aqueous media are in the same range as the values of the fully solvated TEMPO radicals in pure THF. A reduction of the environmental polarity leads to a shift of the electron spin population along the N–O bond in the direction of oxygen and thus to a decrease of a_{iso} as a measure for the unpaired electron spin – ^{14}N nuclear spin coupling strength. The decrease of this value by almost 5 MHz shows that these TEMPO species sense significantly lower ambient polarity, which justifies a denomination as an aqueous lower polarity solvation shell (ALPSS).

A comparison of the data for water and deuterium oxide shows that the fraction f of ALPSS TEMPO probes is significantly increased in D_2O (45.9 % in H_2O vs. 83.4 % in D_2O, see Table 1). This may be due to the higher nuclear mass of deuterium, which leads to a frequency reduction (i.e. a lower zero-point energy) of molecular vibrations of D_2O as compared to H_2O. Moreover, due to the dynamic isotope effect, translational and rotational movements in deuterium oxide are only possible to a significantly lower extent, which is why D_2O shows a 23 % reduced self-diffusion at 25 °C in comparison to H_2O.[21–23] The slightly higher g_{iso}-values in deuterium oxide compared to water can be explained by the absence of H-bonds (the shift of g_{xx} by a single H-bond is estimated to be $\Delta g_{xx} \approx 4\times10^{-4}$, i.e. $\Delta g_{iso} \approx \frac{1}{3}\Delta g_{xx}$, see Eq. S1 ESI†), so beyond these slight changes in H-bonding to the NO-group, the a_{iso}-values indicate a similar polarity in the environment of the spin probes in H_2O and D_2O.[24] We also tested the effect of salt addition to aqueous TEMPO solutions. Referring to the Hofmeister series, which classifies the impact of different ions on hydrophobic effects of macromolecules in water, the addition of an antichaotropic or kosmotropic salt, such as NaCl, should lead to a stabilization of "hydrophobic" interactions.[25–28] In the respective CW EPR spectra at Q-band (see Fig. S9 ESI†) one can see that when increasing amounts of NaCl are added to TEMPO in water, the fraction f_{ALPSS} of the ALPSS TEMPO species also increases. This is also circumstantial evidence that ALPSS TEMPO in fact behave like proteins in nonpolar hydration.

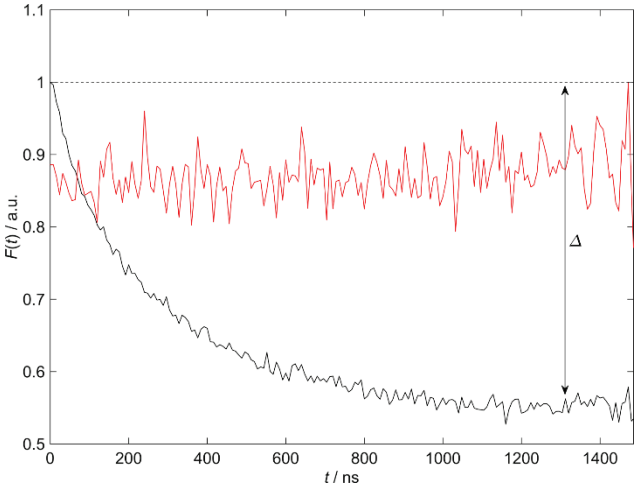

Fig. 2 Background corrected DEER time traces obtained from pulsed X-band measurements of 0.47 mM TEMPO samples in H_2O/10 vol% THF (black) and pure THF (red) at 50 K. For the H_2O/10 vol% THF sample, the modulation depth Δ given in Table 2 is also shown.

To further study a possible effect of the ALPSS on the distribution of TEMPO radicals in water, double electron-electron resonance (DEER) experiments to obtain information on the nanoscale distances/local concentrations (see Fig. 2 and Fig. S6 ESI†) were performed. DEER experiments give a measure of the dipolar interaction between radicals and is often used for nanoscale distance measurements in biophysical and to some degree in materials chemistry.[29,30] Aiming to extract local concentration information, Fig. 2 shows that the background corrected DEER time traces $F(t)$ of TEMPO in the mixture H_2O/10 vol% THF (showing ALPSS even to a higher degree than pure water, see Table 1) and pure THF differ significantly from each other. While in water/10 vol% THF a comparatively strong intensity decay with high modulation depth Δ (see Table 2) can be observed, this is not the case in THF. Note that the sample could be shock-frozen uniformly even without adding additional cryoprotectant, so that for the DEER experiments at cryogenic temperatures (50 K) neither the aqueous mixture with 10 vol% THF nor the pure THF solution contained cryoprotective agents.

The modulation depth of TEMPO in water with $\Delta = 0.440$ corresponds to a value typical for a biradical.[31–34] This and the fact that after Tikhonov regulation the number of spins n_s is about 2, indicates that in aqueous medium a significant fraction of TEMPO probes are locally concentrated in the distance range of about 2–5 nm, whereas in pure THF a completely homogeneous distribution of radicals (and hence little dipolar interaction) can be found. This also explains why especially in the CW Q-band spectra no Heisenberg spin exchange is observed for the "hydrophobic" TEMPO ALPSS species, as this short-range exchange interaction is only effective in a range up to about 1 nm.[35] Nonetheless, combining the information from CW EPR (low polar, aprotic probe environment ALPSS with slowed down rotational dynamics without Heisenberg spin exchange) with that from DEER (much increased local concentration), it seems to be justified to speculate already at this point, that TEMPO and its aqueous lower-polarity solvation shell is locally enriched, i.e. that there is an attractive interaction of ALPSS TEMPO nano-objects that nonetheless do not lead to increased direct collision between the radicals.

Table 2 Modulation depth Δ and number of spins n_s obtained from the background corrected DEER time traces shown in Fig. 2 and Fig. S6 ESI.†

Probe	Solvent	Δ	n_s
TEMPO	H2O/10 vol% THF	0.440	2.08
	THF	0.003	1.28
TEMPONE	H2O/10 vol% THF	0.173	1.46
	THF	0.058	1.32

Simulations of the echo-detected pulse X-band ESE spectra (see Fig. S7 and Table S1 ESI†) also indicate the presence of a bimodal TEMPO spectrum with an ALPSS TEMPO species in the mixture H_2O/10 vol% THF at 50 K. This is visible in the hyperfine splitting constants used and from the broad flanks in the spectra of the aqueous samples that are indicative of dipolar interactions between radicals at distances between 1.5 nm and 2 nm, the distance range between the sensitivities of CW EPR (up to ~1.5 nm) and DEER (above ~1.5–2 nm) .

The nuclear frequency spectra obtained from the Fourier-transformed three pulse electron spin envelope modulation (3p-ESSEM) measurements (see Fig. S8 and Table S2 ESI†) show only solvent-specific ^{1}H-frequencies ($\nu(^1H) \approx 14$ MHz) for TEMPO both in pure THF and in the mixture H_2O/10 vol% THF. Thus, the absence of nitrogen nuclear frequencies ($\nu(^{14}N) \approx 1$ MHz) also supports the interpretation that the ALPSS TEMPO species in aqueous medium do not approach each other sufficiently close for an exchange interaction by radical collisions and SOMO overlap.

Interestingly, the spin probe TEMPONE, which differs from the TEMPO radical in its chemical structure only by the carbonyl group in the 4-position, does not show a second solvated species in its Q- and X-band EPR spectra in water at the same concentration (see Fig. 1E and Fig. S3 ESI†). Furthermore, its CW EPR spectra show a line width approximately half that of TEMPO in water with well-resolved ^{13}C and ^{15}N resonance signals. These significantly smaller line widths in TEMPONE spectra are the constraints on the piperidine ring conformation due to sp^2-hybridization of the carbonyl double bond.[14,36]

As shown in Chart 1, TEMPO, similar to e.g. cyclohexane, most favorably adopts a chair conformation with a mirror plane symmetry of the piperidine ring and an angle α between the N–O bond and the CNC plane of about 19.4°. In contrast, TEMPONE has a twisted ring conformation with a two-fold symmetry axis along the N–O and C=O bond, which are in one plane with the piperidine ring ($\alpha = 0°$).[37] Hence, in TEMPONE the individual dipole moments of these two polar bonds in one plane partially compensate each other, which is why the overall molecular dipole moment μ of TEMPONE ($\mu = 1.36$ D) is significantly lower than that of TEMPO ($\mu = 3.14$ D).[37]

The conformational difference and thus also the different electronic structure of TEMPO and TEMPONE is also seen in the 3p-ESEEM (see Fig. S8 and Table S2 ESI†). 3p-ESEEM as a method allows measurement of relatively weak hyperfine couplings in the radical's environment. While TEMPO shows intense signals in the nuclear frequency spectra at the matrix frequency of hydrogen ($\nu(^1H) \approx 14$ MHz) in H_2O/10 vol% THF as well as in pure THF, TEMPONE shows always much weaker H-signals despite the same concentration. Especially in water the ^{1}H-signal of TEMPONE is considerably smaller compared to TEMPO, indicating a significantly lower isotropic spin density on the 12 methyl protons in α-position. This lower spin density explains the significantly smaller line width of TEMPONE in the CW EPR spectra in comparison to TEMPO, as the unresolved ^{1}H hyperfine couplings of the methyl protons mainly determine the apparent line width. The conformational and electronic differences between the two radicals also lead to different longitudinal nuclear spin relaxation times T_{1n} of the two spin probes (see Table S2 ESI†).

To further characterize the proposed ALPSS and to obtain more information on their stability or transient nature, we performed dynamic light scattering (DLS) and electrospray ionization mass spectrometry (ESI MS) measurements (see Fig. S13–S16 ESI†).

In DLS, the intensity-time correlation function $g_2(t)$ of TEMPO in water is the only one that shows a significantly stronger light scattering compared to the $g_2(t)$-curve of the pure solvent. In all other cases, the correlation functions are almost identical to those observed for the pure solvents. Using a nonlinear CONTIN fit (see ESI† for more details), the hydrodynamic radius r_h (i.e. particle size plus solvation shell) of the scattering particles can be determined from the correlation function $g_2(t)$ of the TEMPO water sample. This results in a bimodal particle size distribution with $r_h \approx 3$ nm and a second quite broad peak ranging from $r_h \approx 20$–228 nm (mean peak position: $r_h \approx 149$ nm) (see Fig. S13 ESI†). While the former short size peak can roughly be interpreted as stemming from individual TEMPO radicals with a "normal" and/or the ALP solvation shells (or maybe low-molecular weight oligomers), the second peak may stem from fuzzy particle cloud locally enriched in ALPSS TEMPO. In particular, the latter picture can excellently be reconciled with the DEER measurements of Fig. 2 and Table 2, in which we see a strong increase in local concentration of TEMPO. From the CW EPR spectra of Fig. 1/Table 1 we additionally know that there is no direct TEMPO-TEMPO collisions, hence combining all these findings allows the conclusion that the TEMPO molecules in the larger structures detected in DLS seem to attract each other while being somewhat shielded from direct collisions through the ALPSS.

In spite of the very different measuring conditions (i.e. detection in the ionized gas phase instead of in solution), the ESI MS measurements remarkably confirm the different behavior of TEMPO and TEMPONE in varying solvents. In ESI MS from aqueous solution, the solvated TEMPO radicals ([M^+] at m/z 156) and larger aggregated species (dimer clusters [$2M^{\cdot}$+Na^+] at m/z 335) are present, which is not the case for TEMPO in THF (see Fig. S14 and S15 ESI†). Furthermore, using the aqueous solution of TEMPONE only solvated radicals ([M^+] at m/z 170) and no larger aggregates, as dimer clusters ([$2M^{\cdot}$+Na^+] expected at m/z 363) are observed. One may interpret this as an indication that during the ESI process apparently amphiphilic TEMPO molecules are in close proximity when they are ionized from aqueous solution (and the water itself is not carried on into the gas phase under these conditions) and hence are detected as dimers, even as the main species. This corroborates the notion of high local concentration of TEMPO in water or aqueous solutions.

At this point, one may already combine the experimental evidence presented to state that, i) there are ALPSS around

TEMPO molecules in water, and that in the same samples ii) an increase of local concentration of TEMPO is found, iii) without leading to direct TEMPO-TEMPO collisions.

Hence, it is desirable to obtain deeper insights into the structure of water in the ALPSS around TEMPO molecules. To this end, we performed force field molecular dynamics simulations of the aqueous solution. One TEMPO molecule was placed in a simulation cell together with 512 water molecules (see ESI† for computational details).[38–45] After equilibration of the density, a production run was performed and evaluated.

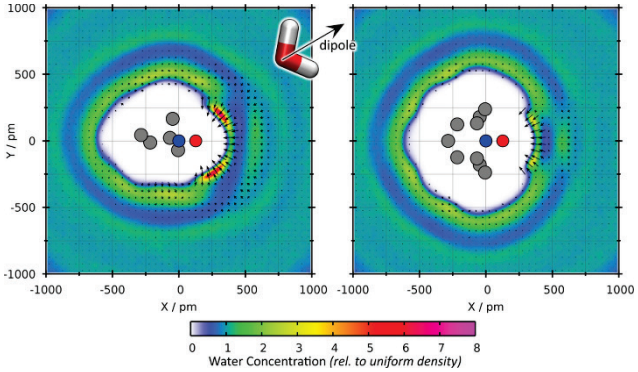

Fig. 3 Computed average water concentration (color scale) and dipole vector orientation (black arrows) around a TEMPO molecule in two different views (left and right). A color scale value of 1 indicates the uniform water density. A clearly separated water layer around TEMPO without preferable dipole orientation (apart from the vicinity of the N–O group) is visible.

In Fig. 3, the average water concentration around the TEMPO molecule in the simulation is presented by the color scale, where a value of 1 corresponds to the uniform density of water. The left and right panel show two different cut planes. It is visible that a clearly separated water layer surrounds the TEMPO molecule (light green), surrounded by a region of low water concentration (blue). The black arrows in the plot depict the average orientation of the water dipole vectors at the respective positions. Apart from the vicinity of the N–O group, which is a strong hydrogen bond acceptor and therefore dictates a clear orientation of the water molecules, it can be seen that there is almost no preferential orientation of dipole vectors in the water layer around TEMPO (i.e. the average over dipole vectors yields the zero vector), which could already indicate a water layer of lower polarity than the one surrounding, e.g. TEMPONE. A similar plot for TEMPONE in water can be found in Fig. S17 ESI.† The results for the water concentration are similar for TEMPONE (clearly separated water layer around the molecule), but as TEMPONE possesses two hydrogen bond acceptors at the opposite sides of the molecule, the dipole vectors of water have a clear preferential orientation at all positions in the water layer, such that the local environment is much more polar here. Overall, Figure 3 may thus be seen as a visual representation of the experimentally deduced ALPSS, as the lack of specific dipole orientation of the water molecules around TEMPO (except for directly at the NO group) can be associated with lower polarity experienced at the radicals' NO groups.

To find out more about the orientation of the water molecules in the ALPSS around TEMPO, we created a two-dimensional histogram, which is presented in Fig. 4. While the horizontal axis depicts the distance *d* between the TEMPO ring center and O(Water), the vertical axis gives the angle *α* between the

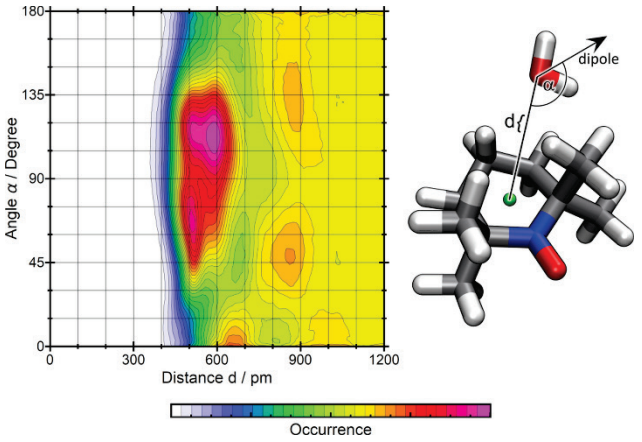

Fig. 4 Two-dimensional histogram showing the orientation of water dipole vectors around TEMPO. Horizontal axis: distance *d* between TEMPO ring center and water oxygen; Vertical axis: angle *α* between connection line from ring center to O(Water) and water dipole vector.

connection line from the ring center to O(Water) and the water dipole vector (see right panel of Fig. 4). It can be clearly seen that at a distance of around 500 pm, which corresponds to the water layer around TEMPO, the angle is in the range of 90° with high preference. In other words, the water dipoles are mostly oriented within the tangent plane of the solvation shell, so that TEMPO does not "see" a dipole moment of the solvent. Such an arrangement of the dipole vectors is typical for a hydrophobic interface of water even macroscopically.[46–48] One may also identify the situation around TEMPO as nonpolar hydration, as it is found in particular in biopolymers, proteins or peptides.[49,50] Here, using CW EPR at higher magnetic fields, one can hence directly measure the local polarity and the remarkably broad polarity range (i.e. low polarity) that pure water can attain when surrounding small amphiphilic molecules.

To investigate a possible aggregation of TEMPO in aqueous solution, we performed force field metadynamics simulations. Two TEMPO molecules were placed in a simulation cell together with 1024 water molecules (see ESI† for computational details).[38–45] After equilibration of the density, a metadynamics simulation with respect to the distance of the two nitrogen atoms was performed. The resulting free energy profiles for TEMPO and TEMPONE are presented in Fig. S18 ESI.† We find a small preference in free energy for aggregation, amounting to around 2 kJ mol^{-1}. However, as the experimental results do not indicate direct aggregation, we conclude that the nonpolar water shells around TEMPO remain intact in these aggregates, so that the TEMPO molecules retain a certain minimum distance.

Conclusions

In this work, multifrequency EPR spectroscopy (X- and Q-band) as intrinsically local measurement technique together with rigorous spectral simulations is used to show that the amphiphilic piperidine-based spin probe molecule TEMPO can build up an aqueous low-polarity solvation shell (ALPSS), whose lower polarity is directly detectable in the Q-band EPR spectra of TEMPO. This species is not observed at standard X-band frequencies but at Q-band frequencies this ALPSS TEMPO species shows a large spectral contrast to the fully solvated TEMPO radicals that are also still recorded in the solution. In a

"better", less polar and aprotic organic solvent, like THF, however, such a behavior of TEMPO is not found. The ALPSS TEMPO does not show Heisenberg spin exchange interaction, indicating that there are now immediate molecular collisions of TEMPO molecules. However, in DEER measurements at X-band in aqueous solution, TEMPO is found not to be homogeneously distributed (unlike in pure THF) but has a locally significantly increased concentration. This local enrichment, estimated by at least a factor of 10, may indicate a kind of local clustering ($n_s \approx 2$, see Table 2). Experimental evidence independent of EPR-spectroscopic measurements for ALPSS TEMPO and local enrichment was obtained in DLS and ESI MS experiments. Furthermore, force field molecular dynamics simulations of the aqueous solution of TEMPO indicates that the solvating water molecules may orient themselves around TEMPO in such a manner to offer an effectively much lower polarity interface towards TEMPO as one may find it in nonpolar hydration e.g. of macromolecules. The such-oriented H_2O molecules may exhibit a relatively long contact time with the enclosed TEMPO radicals and thus form, at least on the EPR time scale (ns–µs), a kind of dynamically formed water layer that we denoted as ALPSS. Thermodynamically, building of ALPSS could be driven by the effort of the comparatively hydrophobic TEMPO probes (*n*-octanol-water partition coefficient $P_{OW} \approx 90$) to minimize the contact surface with the surrounding polar H_2O molecules.[51] This phenomenon, well known as the so-called hydrophobic effect, has already been reported for macromolecular systems (e.g. proteins) and other compounds like carboxylic acids.[49,52,53] In principle, such a behavior can also be observed at every water-air interface, where water minimizes the hydrophobic contact surface (e.g. in the form of a sphere or in the case of gravity in the form of a drop) with the help of its high surface tension. The effect of NaCl addition also has the expected effect of kosmotropic salts, namely increasing nonpolar hydration and hydrophobic interactions.

The TEMPO-surrounding water layer may then prevent the TEMPO probes from getting sufficiently close to each other (i.e. < 1 nm) to exhibit Heisenberg spin exchange interaction. Thus, one has to reconcile a lower polarity solvation on the one hand and an effective attractive interaction between TEMPO molecules without direct TEMPO-TEMPO contacts on the other hand. From our data one may only speculate that the water molecules, especially those ordered around the NO group, may have such a long contact time that effectively TEMPO and its solvation shell act as a dipole that may attract other dipoles (ALPSS TEMPO) and lead to a local enrichment of TEMPO without significantly more frequent direct TEMPO-TEMPO collisions. The observed nanoscopic water-water demixing with a local enrichment of TEMPO radicals may also be regarded as a precursor of macroscopic separation. A deeper insight into the specific nature of the ALPSS, also with regard to the time scale of the H_2O molecule exchange in the solvate envelope, might be provided by other methods, such as NMR.

It should be noted that small amounts of THF seem to be helpful in building ALPSS, very similarly to the effect adding NaCl has. One may speculate that the THF molecules can incorporate to a certain extent into the remaining "gaps" of the H_2O layer solvating TEMPO and thereby stabilize it, e.g. by increasing the contact time of the water molecules. This may then contribute to an increase in the fraction of ALPSS TEMPO species in the Q-band EPR spectra (see Fig. 1C and Table 1).

The dynamic encapsulation of TEMPO molecules in an aqueous lower polarity solvation shell effectively shields the radicals from each other, so that the NO groups cannot collide or even couple with each other. Thus, at spin probe concentrations typical for EPR spectroscopy the formation of the lower polarity solvation species of TEMPO in H_2O and D_2O indeed has a large effect on their environmental polarity and thus on the isotropic hyperfine splitting constant a_{iso}, but does not trigger Heisenberg spin exchange interactions. Only at rather high TEMPO concentrations (i.e. c >> 5 mM) the spin probe density is high enough to observe signal broadening through Heisenberg exchange interactions. Interestingly, if one carefully inspects the concentration dependent Q-band TEMPO spectra (see Fig. S10 ESI†) a significant line broadening (see, e.g., the high-field signal at 30 mM or 40 mM concentration) can mainly be observed for the solvated TEMPO species, but not for the ALPSS TEMPO. This suggests that the dynamic ALPSS can even be seen as a rather robust solvation shell that remains intact or stable when the concentration and hence the collisional frequency of TEMPO is increased.

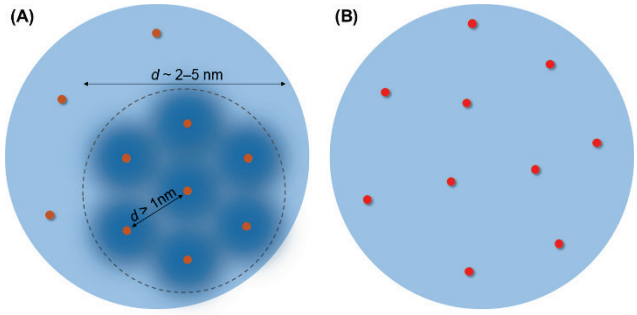

Fig. 5 Schematic depiction of the different solvation behavior of TEMPO (A, orange dots) and TEMPONE (B, red dots) in aqueous medium. While the TEMPONE spin probes are completely homogeneously distributed in aqueous solution, TEMPO shows, besides the fully solvated radicals, another probe species which is surrounded by an aqueous lower polarity solvation shell on the EPR time scale. This ALPSS TEMPO is locally (i.e. in the distance range of approximately 2–5 nm) enriched, as indicated in DEER, DLS and ESI MS experiments. ALPSS prevent spin probe contacts below 1 nm, which would be necessary for a Heisenberg spin exchange interaction that is not observed.

One question that remains and could not be tested so far: why are there in fact two TEMPO species observed in water, the fully solvated and the ALPSS species. At this point, we may merely speculate that despite the rather low initial concentration of less than 0.5 mM, the solvating capacity of water for TEMPO seems to be exhausted already. The concentration series (see Fig S11) of TEMPO in water suggests that there is an equilibrium between the two species that is shifted towards the ALPSS species with higher concentrations. As the Heisenberg spin exchange (and hence collisional) frequency of the fully solvated increases significantly stronger than for the ALPSS TEMPO species, it seems that the entropic penalty for full solvation of TEMPO is the determining thermodynamic factor. This question needs to be addressed in more detail and is beyond the scope of this current initial characterization of the two species.

Taking all facts into account, the different behavior of the two spin probes TEMPO and TEMPONE in the aqueous medium can now be understood better (see Fig. 5). The relatively small (particle diameter parallel to the N–O bond axis $d_{||} \approx 0.79$ nm)

yet dynamic (inversion of chair conformations) and amphiphilic ($P_{OW} \approx 90$) TEMPO radicals with their high dipole moment ($\mu = 3.14$ D) can build up and stabilize an aqueous lower polarity solvation shell.[11,14,37,51] However, in the case of the slightly larger ($d_{||} \approx 0.81$ nm), highly rigid and much more hydrophilic ($P_{OW} \approx 2.3$) TEMPONE probes with a significantly smaller overall dipole moment ($\mu = 1.36$ D), such a shielding process (i.e. the coordination of a solvation shell producing a lower polarity environment) based on nonpolar hydration and the hydrophobic effect, is not necessary (from solvating water molecules' points of view, as due to their stiff twisted ring conformation and two local polar groups a full solvation shell is formed (see Fig. 3 vs. Fig. S17 ESI†).[11,51]

The understanding of the behavior of TEMPO molecules in aqueous solution gained in this paper is of critical importance especially in the field of EPR spectroscopy, since stable TEMPO radicals have been established as spin probes for a long time and are used in many different fields.[8,9,12,13,54,55] In this context, the knowledge of the behavior of TEMPO in aqueous solution or mixtures and its ability to form an aqueous lower polarity solvation shell is of great relevance. It is also an indirect measurement of the incredible flexibility of water when it comes to hydrating amphiphilic substances in nonpolar hydration. Due to the "hydrophobic effect", which can be seen as a direct consequence of such a remarkable solvation shell in aqueous medium, this apparently leads to an inhomogeneous radical distribution through local clustering. From an applications' point of view this probably leads to a less effective energy transfer e.g. in DNP applications, which has already been reported for other nitroxide radicals in aqueous mixtures.[56]

Experimental

For more information on the used materials, methods and computational details see ESI.†

Conflicts of interest

There are no conflicts to declare.

Acknowledgements

The authors thank late Dr. R. Kluge (MLU Halle) for the ESI MS measurements and the research group of Prof. A. Pöppl (Uni Leipzig) for the measurement of a Q-band CW EPR spectrum of an aqueous TEMPO sample. J.H., J.E. and D.H. gratefully acknowledge financial support from the Fonds der Chemischen Industrie (FCI). M.B. acknowledges financial support from the Deutsche Forschungsgemeinschaft (DFG, German Research Foundation) through project Br 5494/1-1.

References

1 O. L. Lebedev and S. N. Kazarnovskii, *Papers on Chemistry and Chemical Technology*, Gor'kii, 1959, p. 649.
2 K.-A. Hansen and J. P. Blinco, *Polym. Chem.*, 2018, **9**, 1479.
3 T. Ono, K. Sato, S. Shimizu, K. Yoshida, T. Dairaku, Y. Suzuki and Y. Kashiwagi, *Electroanalysis*, 2018, **30**, 24.
4 A. Dijksman, A. Marino-Gonzalez, A. M. I. Payeras, I. Arends and R. A. Sheldon, *J. Am. Chem. Soc.*, 2001, **123**, 6826.
5 C. S. Wilcox and A. Pearlman, *Pharmacol. Rev.*, 2008, **60**, 418.
6 V. Chechik and G. Ionita, *Org. Biomol. Chem.*, 2006, **4**, 3505.
7 P. J. Wright and A. M. English, *J. Am. Chem. Soc.*, 2003, **125**, 8655.
8 D. Kurzbach, M. J. N. Junk and D. Hinderberger, *Macromol. Rapid Commun.*, 2013, **34**, 119.
9 J. Hunold, T. Wolf, F. R. Wurm and D. Hinderberger, *Chem. Commun.*, 2019, **55**, 3414.
10 T. Hauenschild and D. Hinderberger, *ChemPlusChem*, 2019, **84**, 43.
11 M. M. Ayhan, G. Casano, H. Karoui, A. Rockenbauer, V. Monnier, M. Hardy, P. Tordo, D. Bardelang and O. Ouari, *Chem. Eur. J.*, 2015, **21**, 16404.
12 L. Song, Z. Liu, P. Kaur, J. M. Esquiaqui, R. I. Hunter, S. Hill, G. M. Smith and G. E. Fanucci, *J. Magn. Reson.*, 2016, **265**, 188.
13 W. A. Braunecker and K. Matyjaszewski, *Prog. Polym. Sci.*, 2007, **32**, 93.
14 J. Lajzerowicz-Bonneteau, in *Spin Labeling: Theory and Applications*, ed. L. J. Berliner, Academic Press, New York, Vol. 1, 1976, pp. 239–249.
15 J. N. Nayak, M. I. Aralaguppi, B. V. K. Naidu, T. M. Aminabhavi, *J. Chem. Eng. Data* 2004, **49**, 468.
16 B. H. Robinson, A. W. Reese, E. Gibbons and C. Mailer, *J. Phys. Chem. B*, 1999, **103**, 5881.
17 B. H. Robinson, C. Mailer and A. W. Reese, *J. Magn. Reson.*, 1999, **138**, 199.
18 B. H. Robinson, C. Mailer and A. W. Reese, *J. Magn. Reson.*, 1999, **138**, 210.
19 R. Chiarelli and A. Rassat, *Tetrahedron*, 1973, **29**, 3639.
20 S. Stoll and A. Schweiger, *J. Magn. Reson.*, 2006, **178**, 42.
21 E. H. Hardy, A. Zygar, M. D. Zeidler, M. Holz and F. D. Sacher, *J. Chem. Phys.*, 2001, **114**, 3174.
22 I. M. Svishchev and P. G. Kusalik, *J. Phys. Chem.*, 1994, **98**, 728.
23 M. Holz, X. Mao, D. Seiferling, A. Sacco, *J. Chem. Phys.* 1996, **104**, 669.
24 Y. Akdogan, J. Heller, H. Zimmermann and D. Hinderberger, *Phys. Chem. Chem. Phys.*, 2010, **12**, 7874.
25 F. Hofmeister, *Arch. Exp. Pathol. Pharmacol.*, 1888, **24**, 247.
26 Y. Zhang and P. S. Cremer, *Curr. Opin. Chem. Biol.*, 2006, **10**, 658.
27 M. Andreev, J. J. de Pablo, A. Chremos and J. F. Douglas, *J. Phys. Chem. B*, 2018, **122**, 4029.
28 A. M. Hyde, S. L. Zultanski, J. H. Waldman, Y.-L. Zhong, M. Shevlin and F. Peng, *Org. Process Res. Dev.*, 2017, **21**, 1355.
29 G. Jeschke, *ChemPhysChem*, 2002, **3**, 927.
30 G. Jeschke, *Annu. Rev. Phys. Chem.*, 2012, **63**, 419.
31 M. J. N. Junk, H. W. Spiess and D. Hinderberger, *J. Magn. Reson.*, 2011, **210**, 210.
32 B. E. Bode, D. Margraf, J. Plackmeyer, G. Dürner, T. F. Prisner and O. Schiemann, *J. Am. Chem. Soc.*, 2007, **129**, 6736.
33 Y. Polyhach, E. Bordignon, R. Tschaggelar, S. Gandra, A. Godt and G. Jeschke, *Phys. Chem. Chem. Phys.*, 2012, **14**, 10762.
34 Y. Polyhach, A. Godt, C. Bauer and G. Jeschke, *J. Magn. Reson.*, 2007, **185**, 118.
35 Y. N. Molin, K. M. Salikhov and K. I. Zamaraev, *Spin Exchange: Principles and Applications in Chemistry and Biology*, Springer, Berlin, 1980.
36 S. R. Burks, M. A. Makowsky, Z. A. Yaffe, C. Hoggle, P. Tsai, S. Muralidharan, M. K. Bowman, J. P. Y. Kao and G. M. Rosen, *J. Org. Chem.*, 2010, **75**, 4737.
37 E. G. Rozantsev, *Free Nitroxyl Radicals*, Plenum Press, New York, 1970, pp. 119–129.
38 L. Martínez, R. Andrade, E. G. Birgin and J. M. Martínez, *J. Comput. Chem.*, 2009, **30**, 2157.
39 C. Vega, J. L. F. Abascal and I. Nezbeda, *J. Chem. Phys.*, 2006, **125**, 034503.

40 E. Stendardo, A. Pedone, P. Cimino, M. C. Menziani, O. Crescenzi and V. Barone, *Phys. Chem. Chem. Phys.*, 2010, **12**, 11697.
41 S. Plimpton, *J. Comput. Phys.*, 1995, **117**, 1.
42 G. J. Martyna, M. L. Klein and M. Tuckerman, *J. Chem. Phys.*, 1992, **97**, 2635.
43 G. Fiorin, M. L. Klein and J. Hénin, *Mol. Phys.*, 2013, **111**, 3345.
44 M. Brehm and B. Kirchner, *J. Chem. Inf. Model.*, 2011, **51**, 2007.
45 W. Humphrey, A. Dalke and K. Schulten, *J. Mol. Graphics*, 1996, **14**, 33.
46 J. Kim, Y. Tian and J. Wu, *J. Phys. Chem. B*, 2015, **119**, 12108.
47 J. Grdadolnik, F. Merzel and F. Avbelj, *Proc. Natl. Acad. Sci. U. S. A.*, 2017, **114**, 322.
48 N. Galamba, *J. Phys. Chem. B*, 2013, **117**, 2153.
49 D. Kurzbach, W. Hassouneh, J. R. McDaniel, E. A. Jaumann, A. Chilkoti and D. Hinderberger, *J. Am. Chem. Soc.*, 2013, **135**, 11299.
50 J. Reichenwallner, C. Schwieger and D. Hinderberger *Polymers*, 2017, **9**, 324.
51 L. J. Kirschenbaum and P. Riesz, *Ultrason. Sonochem.*, 2012, **19**, 1114.
52 N. Islam, M. Flint and S. W. Rick, *J. Chem. Phys.*, 2019, **150**, 014502.
53 T. Gailus, H. Krah, V. Kühnel, A. Rupprecht and U. Kaatze, *J. Chem. Phys.*, 2018, **149**, 244503.
54 J. Hu, N. Whiting and P. Bhattacharya, *J. Phys. Chem. C*, 2018, **122**, 10575.
55 M. Cavaillès, A. Bornet, X. Jaurand, B. Vuichoud, D. Baudouin, M. Baudin, L. Veyre, G. Bodenhausen, J.-N. Dumez, S. Jannin, C. Copéret and C. Thieuleux, *Angew. Chem. Int. Ed.*, 2018, **57**, 7453.
56 E. M. M. Weber, G. Sicoli, H. Vezin, G. Frébourg, D. Abergel, G. Bodenhausen and D. Kurzbach, *Angew. Chem. Int. Ed.*, 2018, **57**, 5171.